Desalination and Water Treatment
www.deswater.com
doi: 10.5004/dwt.2018.22846

130 (2018) 87–97
October

Degradation of isopropyl ethylthionocarbamate from aqueous solution by Fenton oxidation: RSM optimization, mechanisms, and kinetic analysis

Donghui Liu[a,b], Guohua Gu[b,c*], Bichao Wu[b,c*], Chongqing Wang[d,e], Xiong Chen[b,c]

[a]*School of Economics and Management, China University of Geosciences, Beijing 100083, China, email: mary_ldh16@163.com*

[b]*School of Minerals Processing and Bioengineering, Central South University, Changsha 410083, Hunan, China, emails: guguohua@126.com (G. Gu), wu_bi_chao@163.com (B. Wu), 1428105545@qq.com (X. Chen)*

[c]*Key Laboratory of Hunan Province for Clean and Efficient Utilization of Strategic Calcium-containing Mineral Resources, Central South University, Changsha 410083, China*

[d]*Key Laboratory of Resources Chemistry of Nonferrous Metals, School of Chemistry and Chemical Engineering, Central South University, Changsha 410083, Hunan, China, emails: 786252819@qq.com, zilangwang@126.com*

[e]*School of Chemical Engineering and Energy, Zhengzhou University, Zhengzhou 450001, China*

Received 2 December 2016; Accepted 22 July 2018

ABSTRACT

Efficiency in chemical degradation of isopropyl ethylthionocarbamate (also referred as Z-200) using Fenton reagents was studied in this paper. A Box–Behnken design method with response surface methodology (RSM) was used to investigate the influence of individual and interaction of operating variables on removal efficiency with the aim of recognizing the optimum operating conditions. The mechanism of oxidation degradation was further examined by Fourier transform-infrared spectroscopy, and gas chromatography coupled with mass spectrometry. The optimum conditions for chemical degradation efficiency of Z-200 were obtained as Fe^{2+} 146 mg/L, H_2O_2 98 mg/L, and initial pH 6.7, achieving a removal efficiency of 92.76% in a 2.5 h reaction time. Finally, a simple kinetic analysis was carried out based on the degradation of Z-200 at different concentrations. Results showed that the kinetics of the Z-200 degradation rate followed pseudo-first-order equation in Fenton process. This study effectively demonstrated the usage and advantages of RSM for the modeling and prediction of process response. It also can be revealed that the advanced oxidation process of Fenton is an effective and efficient technology for the degradation of Z-200 in aqueous solution.

Keywords: Fenton oxidation; Isopropyl ethylthionocarbamate; Degradation; Response surface methodology (RSM); Kinetic analysis

1. Introduction

O-Isopropyl-*N*-ethylthionocarbamate (trade-marked Z-200) has been widely used as a collector in ore dressing plant for decades, which is especially recommended for the flotation of copper minerals because of its excellent selectivity against pyrite in alkaline media [1,2]. More importantly, new ester collectors that have comparable properties as Z-200 have been increasingly produced to apply in concentrators. However, even a small concentration of these reagents in water streams is toxic to water life and have high chemical organic demand in the discharge of wastewater [3–5]. Additionally, Z-200 has been investigated that it could break down and produce by-products of COS and CS_2 during degradation when irradiated by ultraviolet light [6]. According to the literature, Z-200 is hardly biodegradable and it also cannot be degraded by conventional chelating or coagulation settlement. Removal of Z-200 through anaerobic digested sludge has once been studied by Chen [7]. The high degradation rate needs longer processing period and moderate medium must be added to obtain excellent development of bacteria. So far, there are few reports on the removal of Z-200. Hence, removal of Z-200 with high efficiency and no secondary products, which requires more studies, is significant from an environmental viewpoint.

* Corresponding author.

In present decades, advanced oxidation processes (AOPs) have usually been utilized to treat various refractory organic compounds as eco-friend technologies especially when traditional methods are not effective [8]. Hydroxyl radical (•OH) plays the key role in AOPs and it is the strongest (E^0 = 2.80 V) oxidant of reactive oxygen species, which can attack various pollutants unselectively and efficiently [9–12]. The simplest and most effective way of generating hydroxyl radicals is by Fenton reaction and it has attracted broad attention among the AOPs due to its strongly oxidative ability for the degradation of organic pollutants [13]. The generally accepted chain reactions are shown as follows [10,14,15]:

$$Fe^{2+} + H_2O_2 \rightarrow Fe^{3+} + {}^{\bullet}OH + OH^- \quad (1)$$

$$Fe^{3+} + H_2O_2 \rightarrow Fe^{2+} + HO_2^{\bullet} + H^+ \quad (2)$$

Hydroxyl radical is generated via the decomposition of H_2O_2 catalyzed by Fe(II). Due to the efficiency of treatment and simple oxidation process, Fenton reagent has been widely used to oxidize and mineralize organic compounds for the treatment of various contaminants, such as agricultural wastewater [16], pharmaceutical wastewater [17,18], cosmetic wastewater [19], dye wastewater [20], and municipal wastewater [21]. Since it is the hydroxyl radical that really works, more and more researchers devote themselves to optimizing the Fenton system to generate more hydroxyl radical to treat wastewater more efficiently.

In general, the activity of catalyst in Fenton systems or Fenton-like systems is higher at acid or neutral pH than at alkaline pH. The efficiency of degradation was considerably improved as temperature increased. Perini et al. [22] evaluated the pH limitation by the use of low iron concentrations and organic ligands, the highest total organic carbon (TOC) removal (0.87) was achieved at pH 4.5. Feng et al. [23] studied the effect of initial solution pH on the degradation of Orange II in photo-Fenton systems. The results showed that the best photo-catalytic activity occurred at an initial solution pH of 3.0. Furthermore, a reasonable efficiency of degradation could be obtained at an initial solution pH of 6.6. Zazo et al. [24] investigated the effect of temperature on the treatment of phenol by the Fenton process within the range of 25°C–130°C, a reduction of almost 80% was obtained at 90°C, while at 25°C the TOC decreased less than 28%. Kan and Huling [25] explored the effects of temperature (25°C, 35°C, 45°C, and 55°C) on Fenton-driven chemical oxidation of methyl *tert*-butyl ether, the activity of catalyst was also improved as the temperature increased.

Recently, many statistical experimental design methods have been developed for process optimization. These methods involve using mathematical models for designing chemical processes and analyzing the process results [26]. Recently, response surface methodology (RSM), which is a collection of statistical techniques used to develop, improve, and optimize processes, has been widely used in many fields. There are many published researches on wastewater treatment using RSM optimization processing [27–29]. RSM tool is useful in predicting the effect of individual experimental factors, as well as locating interactions between the factors. Also, it is the most economical method for characterizing a complicated experimental process. It requires fewer experiments to determine the optimum conditions. The regularity of experimental results can be clearly described by a function equation or 3D graphs or contour maps in RSM design. Therefore, RSM was used in this study.

The objectives of this study were to: (1) optimize the various operational parameters on the degradation of Z-200 by Fenton degradation and find the most suitable combination of variables resulting in the maximum Z-200 removal efficiency, using the RSM based on Box–Behnken design (BBD); (2) explore the possible mechanisms during Fenton oxidation and determine whether some by-products are generated in Fenton reaction, employing the measurements of Fourier transform-infrared (FT-IR) spectroscopy and gas chromatography coupled with mass spectrometry (GC-MS); (3) treat the different concentrations of Z-200 under the optimum condition which is determined by RSM above and extensively investigate the oxidation kinetics at different concentrations.

2. Materials and methods

2.1. Chemicals and reagents

Z-200 was purchased from Zhuzhou Flotation Reagents Factory, China. Z-200 was of technical grade and used without purification. Fe^{2+} in the Fenton's reagent was prepared from $FeSO_4{\cdot}7H_2O$ (analytical grade, Sinopharm Chemical Reagent, China) and H_2O_2 (30 wt%, Sinopharm Chemical Reagent, China) was of analytical grade. Analytical grade H_2SO_4 (40 wt%, Xinyang Chemical Company, China) and NaOH (40 wt%, Xinyang Chemical Company, China) were adjusted to the desired initial pH before Fenton's reagent. All reagents were used as received. The solutions were prepared with distilled water. The initial concentration of Z-200 was 0.5 g/L, then the solution was diluted to other concentrations.

2.2. Experimental procedure

Z-200 water samples used in the oxidation experiment were diluted from 500 to 20 mg/L for the RSM optimization process and to different concentrations (10, 20, 70, and 100 mg/L) for the kinetic analysis. First, pH value of solution was controlled and a certain amount of Fe^{2+} was added into 200 mL Z-200 water samples. Then the given amount of H_2O_2 was consequently added, under a stirring speed of 300 rpm for 10 min. All of the above processes were carried out in a 300 mL beaker with a single-paddle gang stirrer at room temperature. After deposited for the given time, the sample solution was taken from beakers and filtered through the qualitative filter paper (aperture: 12–25 μm; Ø = 15 cm) with medium speed, then analyses by UV or GC-MS were conducted. As for FT-IR analysis, the products before and after oxidation of Z-200 sample were mixed with hexane separately and were shaken for a few minutes. Then the organic phase was extracted and measured by FT-IR after centrifuging for 10 min.

2.3. Techniques and analysis

Determination of the concentration of Z-200 (characteristic of ultraviolet absorption peak at 241 nm) was

achieved by UV–vis spectrophotometer (UV-2100, Shimadzu Corporation, Japan), and a coefficient of determination of 0.99997 was observed, which exhibited a good linearity. In order to examine the mechanism of oxidation process, the products before and after oxidation were measured by a FT-IR spectrometer of Nicolet 6700 (Nicolet Corporation, America) and GCMS-QP2010 (with electron ionization (EI), Shimadzu Corporation, Japan). Chromatograph was equipped with 30 m × 0.25 mm i.d. DB-5 ms capillary column of 0.25 μm film thickness. Helium 5.0 was used as the carrier gas. The experiments were carried out at a starting temperature of 160°C, and then temperature was increased 20°C/min up to 300°C. Temperature of both GC oven and injector was 280°C. All the injections were made in split mode. The standard NIST 11 mass spectral library database was used to identify the organic compounds. The solution pH was analyzed by a portable pH meter PHS-3C (Shanghai Leici Corporation, China).

2.4. RSM design

In this experiment, a three-factor, three-level factorial BBD was selected to model and optimize the degradation process of Z-200. Z-200 removal efficiency (Y) was taken as response of the system. Initial pH (X_1), dosage of Fe_2SO_4 (X_2, mg/L), and dosage of H_2O_2 (X_3, mg/L) were chosen as three independent variables. The three independent variables and their ranges in coded and actual values were listed in Table 1. Results from all BBD experimental runs were analyzed by the least-squares regression method to predict the process response and to estimate the coefficients according to the following second-order Eq. (3), which was carried out to describe the mathematical relationship between the predicted response (Y) and input variables (X_1, X_2, and X_3) in coded values:

$$Y = \beta_0 + \sum \beta_i X_i + \sum \beta_{ii} X_i^2 + \sum \beta_{ij} X_{ij} \quad (3)$$

where Y refers to the predicted response associated with each factor level combination by the model; β_0 is the model constant (intercept term), β_i, β_{ii}, and β_{ij} are the linear, quadratic, and interaction coefficients, respectively. Additionally, the ranges of the variables and the removal efficiency after 150 min of reaction were considered based on the preliminary experiments.

The experimental data were analyzed via Design Expert software version 8.0.6 (STAT-EASE Inc., Minneapolis, USA) for the analysis of variance (ANOVA) and to assess the goodness of fit of the model.

3. Results and discussion

3.1. Model fitting and statistical analysis

Table 2 presents the complete experimental design matrix as suggested by Design-Expert Software along with response values obtained from the experimental works. According to experimental data, the following fitting polynomial equation (4) was obtained from data fitting as follows:

$$Y = 90.84 + 0.90X_1 + 10.58X_2 - 2.16X_3 + 1.49X_1X_2 + 1.69X_1X_3 - X_2X_3 - 3.63X_1^2 - 13X_2^2 - 2.13X_3^2 \quad (4)$$

Table 1
Experimental range and levels of the independent variables

Independent variables	Codes	Ranges and levels		
		−1	0	+1
Initial pH	X_1	3.5	6.5	9.5
Fe^{2+} dosage(mg/L)	X_2	60	120	180
H_2O_2 dosage(mg/L)	X_3	60	150	240

Table 2
BBD matrix and corresponding experimental responses

Runs	X_1	X_2 (mg/L)	X_3 (mg/L)	Z-200 removal (%)
1	6.5	120	150	90.50208
2	3.5	120	60	88.04871
3	6.5	60	240	63.02434
4	3.5	60	150	63.73309
5	6.5	180	60	90.39304
6	6.5	120	150	92.2467
7	9.5	120	240	85.4863
8	6.5	120	150	89.79333
9	9.5	60	150	64.00569
10	3.5	120	240	81.76391
11	6.5	120	150	90.62988
12	9.5	180	150	87.67456
13	9.5	120	60	84.99288
14	3.5	180	150	81.43554
15	6.5	120	150	91.01298
16	6.5	180	240	82.63956
17	6.5	60	60	66.76839

where Y is the removal efficiency for Z-200, X_1, X_2, and X_3 are the coded values of three independent variables described above. A positive sign in front of the terms indicates synergistic effect, whereas a negative sign indicates antagonistic effect [30].

Diagnostic plots, such as predicted versus actual values, were used to determine the adequacy of the model. The predicted values of Z-200 removal were calculated using the regression model and compared with experimental values in Fig. 1. As can be seen, the experimental results were in good correlation with the values predicted by statistical model, thus validating the predicted model [31].

Furthermore, adequacy of the obtained model to predict the Z-200 removal efficiency was analyzed through the ANOVA and the results are expressed in Table 3. Results show that this quadratic model is highly significant, implied by the high F-test values (115.79) with the very low probability value (Prob. > F < 0.0001). In addition, the Lack-of-Fit, F-value, 3.59, (F < 4.7725) implies that the shortage of the proposed model in the prediction of response factor is insignificant, thus confirming the model adequacy. Also, the adequate precision ratio of 27.634 (>4) indicates an adequate signal for the quadratic model. In addition, a coefficient of variance of 1.6% (<10%) indicates the high accuracy and reliability of the experiment [32–34]. The values of R^2 and adjusted R^2 for reduced model are 0.9933 and 0.9847, respectively,

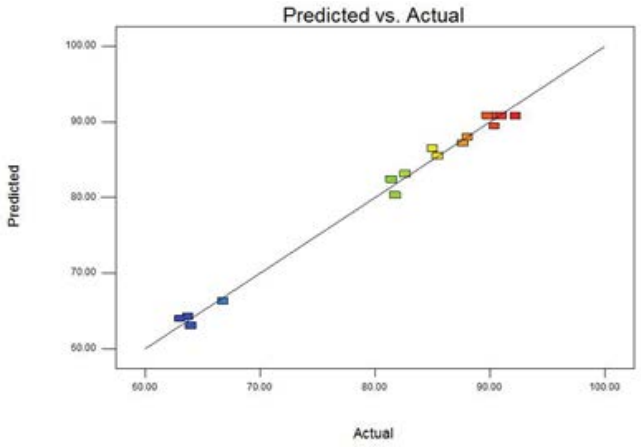

Fig. 1. Design expert plot: actual values versus predicted response by BBD.

Table 3
ANOVA for response surface quadratic model

F value	115.7897	*P* value	<0.0001
Lack of fit (*F*)	3.59	Lack of fit (*P*)	0.1245
R^2	0.9933	R^2_{adj}	0.9847
CV %	1.6	Adeq precisor	27.634

which has satisfactory agreement between them, indicating that the unnecessary variables are not included in the model [35]. Therefore, it is noticeable that the selected model is suitable for navigating the design space.

3.2. Interactions among the factors and optimization results

The 3D response surface and 2D contour plots shown as graphical representations were applied to show the interactive effects of operational parameters on degradation efficiency of Z-200. Fig. 2(a) shows the response surface and the corresponding contour of the combined effect of pH and Fe^{2+}, while H_2O_2 is maintained at certain dosage. From response surface curves and contours, it is easy to understand the interaction effects between two independent variables and also to locate the optimum levels. Compared with the influence of pH on Z-200 removal, the concentration of Fe^{2+} has greater effect on degradation of Z-200. Z-200 removal improved with Fe^{2+} concentration increased to 146 mg/L, for certain amount of •OH could be generated by enough Fe^{2+} dosage according to reaction (1). Nevertheless, higher concentration of Fe^{2+} (>146 mg/L) inhibited the generation of •OH. Because excessive Fe^{2+} concentration favor the occurrence of the scavenging reaction (5) as follows:

$$Fe^{2+} + {}^{\bullet}OH \rightarrow Fe^{3+} + OH^- \quad (5)$$

Fig. 2(b) shows the response surface and the corresponding contour of the combined effect of pH and H_2O_2, while Fe^{2+} is maintained at a certain dosage. According to the contour, there is a significant interaction between pH and H_2O_2. At the optimum level of both pH and H_2O_2, the best removal efficiency could be achieved. At lower or higher pH values, a significant decrease in the efficiency of the process was observed. At low pH (<2), H_2O_2 is stabilized as $H_3O_2^+$ [36], the reaction between $OH^{\bullet}$ and H^+ becomes dominant [37] and the regeneration of Fe^{2+} by reaction of Fe^{3+} with H_2O_2 will be inhibited [38]. In alkaline conditions, the precipitation of Fe^{3+} ($Fe(OH)_3$) could hinder the reaction between Fe^{3+} and H_2O_2 to inhibit the regeneration of Fe^{2+}. Besides, $Fe(OH)_3$ leads to the decomposition of H_2O_2 to O_2 and H_2O, thus decreasing the production of $OH^{\bullet}$ [39]. As can be seen from the contour, a higher level beyond the optimum dosage of H_2O_2 has significantly negative effect on Z-200 removal, which is due to the reaction between H_2O_2 and •OH, hence, Z-200 cannot be oxidized. Nevertheless, the optimum initial pH value is relatively higher than many studies reported, as the optimum initial pH values may be determined by target organic compounds. Additionally, no buffering effects were observed in the sample Z-200 solution, and therefore the addition of Fe^{2+} and H_2O_2 could decrease the solution pH.

Fig. 2(c) shows the response surface and the corresponding contour of the combined effect of $Fe^{2+}$and H_2O_2, while pH is maintained at certain level. As can be seen in the figure, the optimum combined levels between $Fe^{2+}$and H_2O_2 can be located. According to many studies, the optimum ratio between Fe^{2+} and H_2O_2 plays a key role in the oxidation process and the ratios may vary from compounds to compounds [19]. The precise optimum ratio can be found by the use of RSM design.

Based on the analysis by design-expert, optimization results were achieved to evaluate the optimal experimental parameters for Z-200 removal. Table 4 shows the optimum conditions based on combination of all the response surfaces and their corresponding contours. Under the optimum conditions (pH: 6.7, Fe^{2+}: 146 mg/L, H_2O_2: 98 mg/L), a removal efficiency of 92.76% was achieved within 2.5 h of reaction time. Only small deviations (1.1%) were found between the experimental values and the predicted values. Thus, the BBD model can be used to optimize the process of Z-200 removal.

3.3. FT-IR and GC-MS analysis

3.3.1. FT-IR analysis

The FT-IR spectra are recorded as a qualitative analysis to determine the main functional groups. The FT-IR spectra of Z-200 sample and oxidation product are shown in Fig. 3. According to Fig. 3(a), absorption peaks of 2,961.86 and 2,874.25 cm^{-1} are derived from the $–CH_3$ asymmetry and symmetry stretching vibration. Peaks at 1,456.98 and 1,377.64 cm^{-1} contribute to asymmetry and symmetry bend vibration of $–CH_3$, and peaks at 2,926.14 and 1,456.98 cm^{-1} are $–CH_2–$ asymmetry stretching vibration and bend vibration, respectively. Peaks at 3,251.59, 1,209.64, and 1,054.89 cm^{-1} are caused by vibrations of –NH–, C–N from secondary amine, and C–O from formic acid ester, respectively. Peaks at 1,515.27, 1,397.58, 1,097.81, and 964.85 cm^{-1} are characterized by a coupled vibration between C=S and C–N. IR characteristic peaks described above showed an exact agreement with the chemical group of the structure of Z-200 ($CH(CH_3)_2OSCNHC_2H_5$) [40,41].

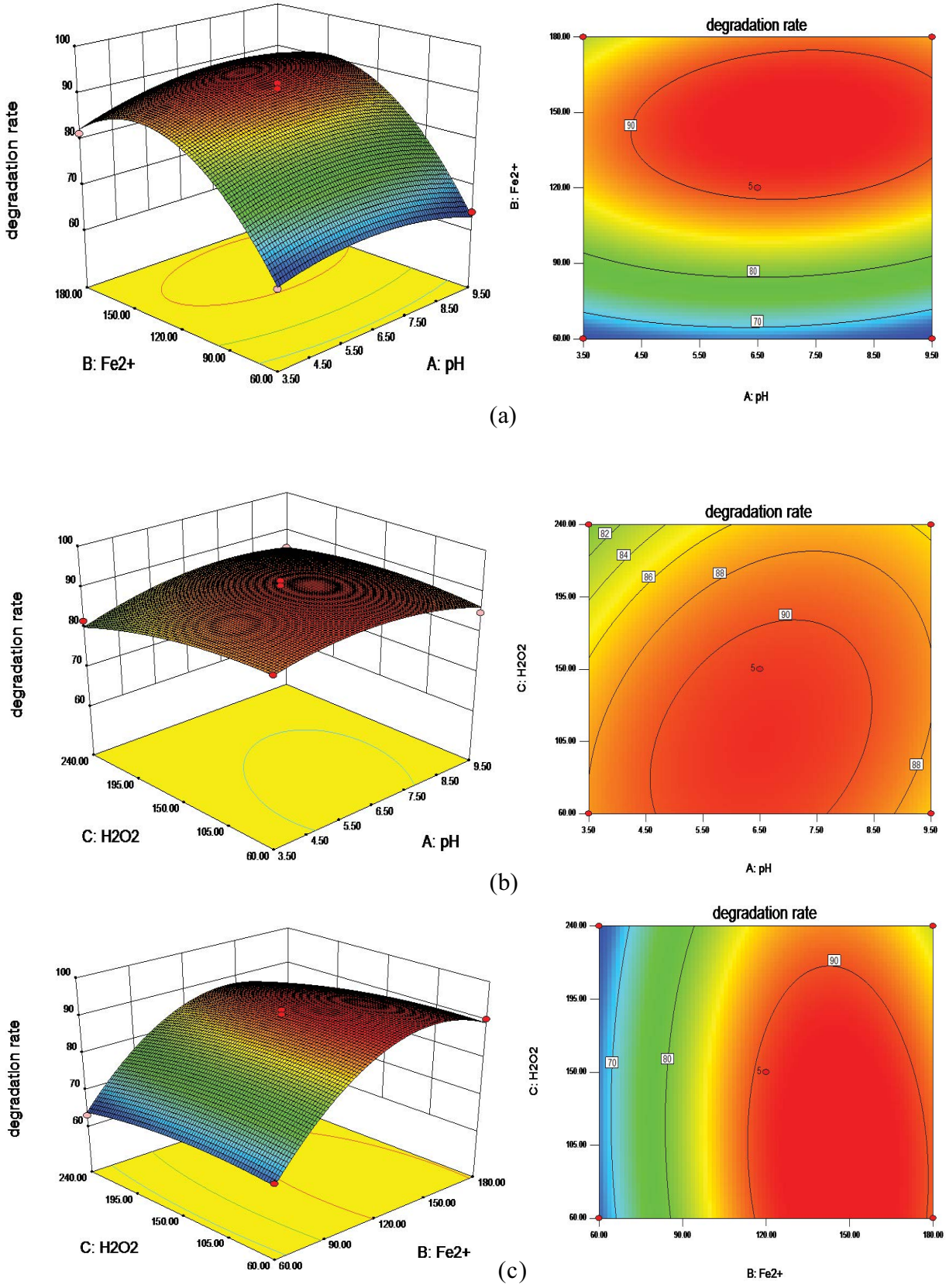

Fig. 2. Response surface plots and contours for Z-200 removal efficiency as a function of (a) Fe^{2+} dosage and pH, (b) pH and H_2O_2 dosage, and (c) Fe^{2+} dosage and H_2O_2 dosage.

Table 4
Predicted and experimental values of the responses at optimum conditions

Initial pH	Fe^{2+} dosage (mg/L)	H_2O_2 dosage (mg/L)	Z-200 degradation rate	
			Predicted value	Experimental value[a]
6.74	146	98	93.7886	92.76

[a]The experimental value was the average of three parallel experiments.

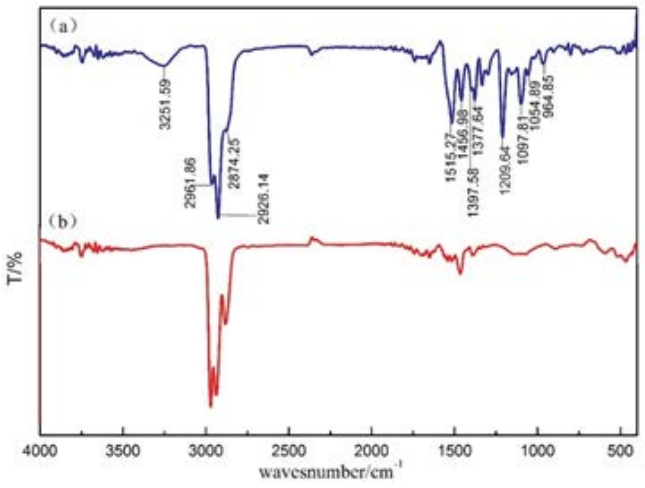

Fig. 3. Infrared spectrum scan of Z-200 before and after oxidation degradation ((a) sample of Z-200 before oxidation, (b) sample of Z-200 after Fenton oxidation).

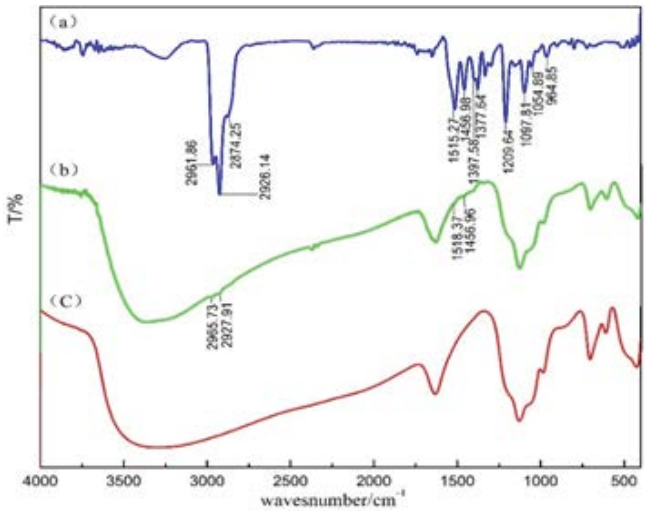

Fig. 4. Infrared spectrum scan of (a) Z-200 before oxidation, (b) flocs produced in the oxidation process of Z-200 sample, and (c) flocs produced in the blank experiment.

As can be seen from Fig. 3(b), there are characteristic absorption peaks of $–CH_3$ and $–CH_2–$ remained after oxidation (peaks at 2,961.86, 2,874.25, 2,926.14, and 1,463.73 cm^{-1}), mainly due to the hydrocarbon impacts of extraction agent of *n*-hexane. It can be observed that the characteristic absorption peaks of Z-200 completely disappear after Fenton oxidation, which indicates that Z-200 was effectively degraded and moreover no significant by-products were produced. As flocs could be produced during Fenton oxidation, the flocs were also measured by FT-IR. Distilled water treated with Fenton reagent was also carried out, which acted as blank experiment. Fig. 4(c) shows the IR spectrum scan of the flocs produced in the blank experiment. As illustrated in Fig. 4(b), there appear some weak characteristic absorption peaks in the scan of flocs after Fenton oxidation, which indicates that flocculation also works in the whole process of Fenton treatment but only a weak supporting role.

3.3.2. GC-MS analysis

Z-200 sample and products after oxidation were analyzed by GC-MS to further evaluate their compositions. Fig. 5 shows the total ion chromatography (TIC) spectrum of Z-200 sample and products after oxidation. According to the NIST 11 mass spectral library database, the main components of Z-200 sample were identified and are shown in Table 3 (the spectrums of MS for each peak are shown in the supplementary material). It can be observed that Z-200 marked C in Table 5 was almost completely degraded by Fenton oxidation where the retention time was 4.747. After oxidation treatment, the relative abundance of Z-200 was significantly reduced, whereas other products which acted as by-products during Z-200 production were not effectively degraded. According to Fig. 5, there are no significantly secondary products after Fenton oxidation. It can be revealed that Fenton tend to be a better method to degrade Z-200 without significant by-products [42].

3.4. Treatment of different concentrations of Z-200 and kinetic analysis

The dosage of Z-200 using as collector in factories may vary from minerals to minerals, and moreover the concentrations may vary according to the specific situations. Hence, it is important to investigate the removal of different concentrations of Z-200. The various concentrations were also degraded by Fenton oxidation under the optimum conditions which were determined by RSM design earlier. Results are shown in Fig. 6. As illustrated in the figure, Z-200 at low concentrations can be effectively degraded in a shorter time, and there exists no significant improvement with the increment of time. Whereas Z-200 at high concentrations is slightly degraded within short time, however, it gains extremely significant improvement with the increment of time. When the reaction time is above 3 d, the degradation rate can be beyond 95% at all concentrations. This phenomenon may be

Table 5
Results of the GC-MS analyses of the main organic components of Z-200 sample

Number	Retention time (min)	Compounds	Molecular formula
A	3.931	1-Octanol	$C_8H_{18}O$
B	4.106	Ethene, methoxy-	C_3H_6O
C	4.747	Ethylcarbamothioic acid, *O*-isopropyl ester	$C_6H_{13}NOS$
D	5.140	4(1H)-Pyrimidinone, 2-(methylthio)-	$C_5H_6N_2OS$
E	5.490	Benzene, (1,2-dichloroethyl)-	$C_8H_8C_{l2}$
F	5.969	Benzamide	C_7H_7NO
G	6.507	Phosphoric acid, diheptyl methyl ester	$C_9H_{20}FO_2$
H	6.738	5,6-Dichloro-2-[4-[2-diethylamino]propyl]amino-6-methylpyrimidin-2-ylamino-1H-benzimidazole	$C_6H_{10}N_2O$
I	7.882	Tributyl phosphate	$C_{12}H_{27}O_4$

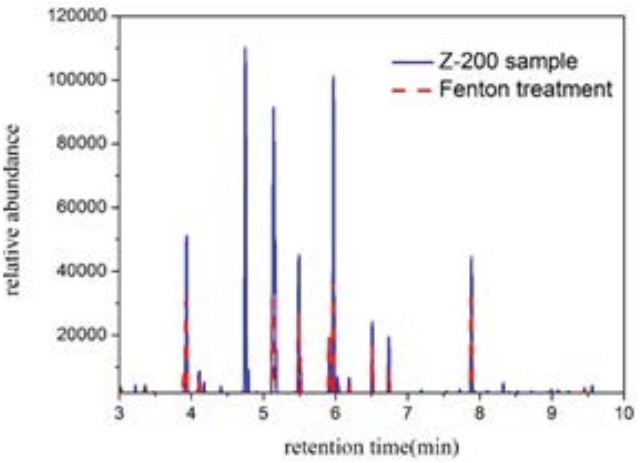

Fig. 5. GC-MS TIC spectrum of Z-200 before and after oxidation.

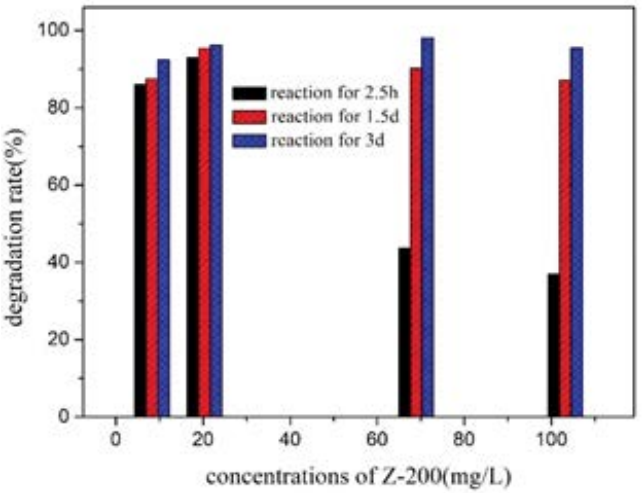

Fig. 6. Treatment of different concentrations of Z-200 under optimum conditions determined by RSM design. (Conditions: Z-200 20 mg/L, Fe^{2+} 146 mg/L, H_2O_2 98 mg/L, solution initial pH 6.74).

due to the reaction between organic matters and Fe^{3+}, which is illustrated as follows:

$$Fe^{3+} + {}^{\bullet}R \rightarrow Fe^{2+} + R^{+} \quad (6)$$

The reproduce of Fe^{2+} results in more $^{\bullet}OH$ according to reaction (1), which enhances the degradation in the following time [43–45]. As time passes, Fe^{2+} continues to be generated to achieve a better degradation of target organic compounds.

To further investigate the comprehensive reaction system of Z-200 removal, the kinetic analysis was carried out at different concentrations [11]. The degradation kinetics of the Fenton oxidation step was expressed in terms of Z-200 removal under the optimum conditions established in the RSM design. In this study, two phases were divided to separately research, one phase was during reaction time before 3 h, and another was during reaction time after 1 d. There was a linear region in plots of $\ln(C_0/C)$ versus time. The slope of the line was used to obtain the rate constant, the degradation process using the pseudo-first-order rate expression is as follows:

$$\ln C_t = \ln C_0 - kt \quad (7)$$

where t is the reaction time, C_0 and C_t are the concentration of Z-200 at time zero and time t, respectively, and k is the rate constant. The kinetic plots are given in Fig. 7.

Fig. 7 shows that pseudo-first-order kinetic equations can accurately describe the degradation of Z-200 in specific course of oxidation process. Z-200 at high concentrations had a slower rate constant within 3 h, whereas Z-200 at low concentrations had the opposite behavior. On the other hand, the rate constant became the lowest level when Z-200 at 20 mg/L in the longer oxidation process. There existed extreme change of the rate constant of Z-200 at high concentrations. The phenomenon above corresponded well with the results in Fig. 6. The results indicated that oxidation treatment technology can be applied extensively in various concentrations of Z-200 removal, and the higher concentrations of Z-200 can also be effectively degraded if the reaction time is increased.

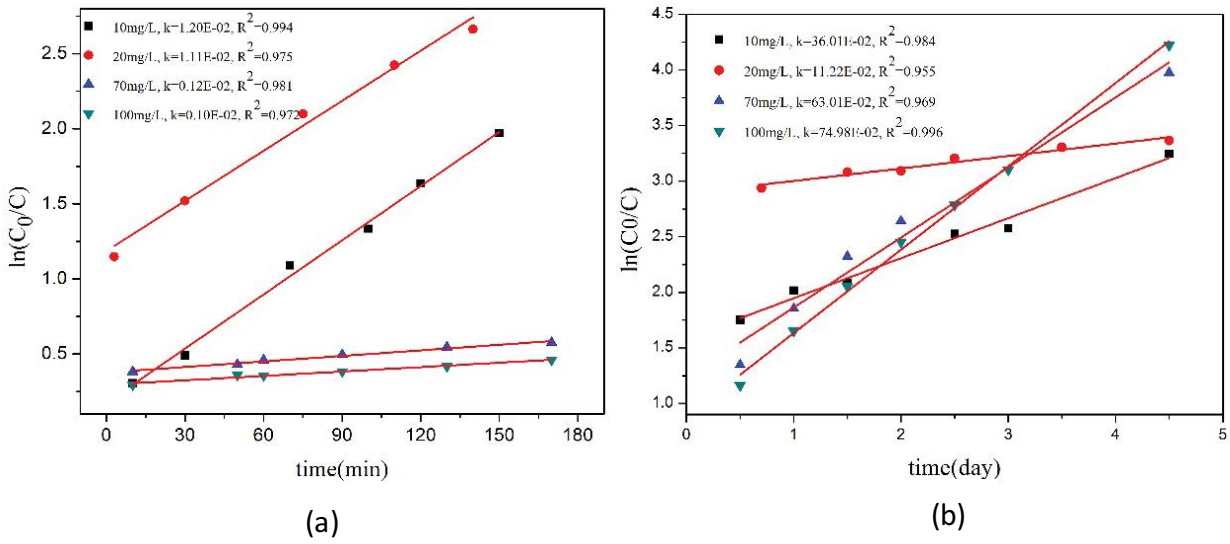

Fig. 7. Degradation kinetics of Z-200 oxidation process (a) within 3 h, (b) after half a day.

4. Conclusions

In this study, the optimization of Z-200 removal efficiency, using an experimental design methodology was studied. The BBD based on RSM was successfully used to model and predict the effects of Z-200 removal by Fenton oxidation. Under the optimized conditions of initial pH 6.74, Fe^{2+} dosage 146 mg/L, and H_2O_2 dosage 98 mg/L, degradation rate can reach 92.76% with the reaction time of 2.5 h. The concentration of Z-200 can be reduced by Fenton to a level which has no damage to environment.

Compared with other treatment of Z-200, IR spectroscopy and GC-MS analysis showed that no significant by-products would be generated during Fenton oxidation process, which indicated that Z-200 can be almost completely degraded by Fenton reagents and can be oxidized to CO_2, H_2O, NH_3, etc. eventually. This method can be efficiently and eco-friendly used in the wastewater treatment.

Z-200 at different concentrations can also be degraded by Fenton reagent under optimum conditions which was determined by RSM design. The higher concentrations of Z-200 can be effectively degraded under longer reaction time. Degradation process can be described as the pseudo-first-order reaction kinetics equation, which can provide a theoretical basis and technical guidance for treatment of actual wastewater plant.

Acknowledgments

The authors gratefully acknowledge the financial support by the National Science-technology Support Plan (no. 2015BAB12B02); and the National Natural Science Foundation of China (no. 51374249); and the Guangdong provincial science and technology plan (no. 2013B090800016); the Key Laboratory of Hunan Province for Clean and Efficient Utilization of Strategic Calcium-containing Mineral Resources (no. 2018TP1002); and the Fundamental Research Funds for the Central Universities of Central South University (no. 2018zzts800).

References

[1] A.N. Buckley, G.A. Hope, K.C. Lee, E.A. Petrovic, R. Woods, Adsorption of O-isopropyl-N-ethyl thionocarbamate on Cu sulfide ore minerals, Miner. Eng., 69 (2014) 120–132.
[2] R. Crozier, Flotation: Theory, Reagents and Ore Testing, Pergamon Press, Oxford, 1992, pp. 62–64.
[3] E. Chockalingam, S. Subramanian, K.A. Natarajan, Studies on biodegradation of organic flotation collectors using *Bacillus polymyxa*, Hydrometallurgy, 71 (2003) 249–256.
[4] S.H. Chen, W.Q. Gong, G.J. Mei, Q. Zhou, C.P. Bai, N. Xu, Primary biodegradation of sulfide mineral flotation collectors, Miner. Eng., 24 (2011) 953–955.
[5] X.M. Jie, H. Wang, Y. Chen, Removal of dianiline dithiophosphoric acid from wastewater by chelate precipitation, Desal. Wat. Treat., 57 (2016) 5100–5107.
[6] C.X. Chen, Research on Second Pollution of Mine Sulfur Beneficiation Reagents and Testing Measurements, Guilin University of Technology, Guangxi, China, 2008.
[7] S.H. Chen, W.Q. Gong, G.J. Mei, W.Y. Han, Anaerobic biodegradation of ethylthionocarbamate by the mixed bacteria under various electron acceptor conditions, Bioresour. Technol., 102 (2011) 10772–10775.
[8] C.D. Qi, X.T. Liu, J. Ma, C.Y. Lin, X.W. Li, H.J. Zhang, Activation of peroxymonosulfate by base: Implications for the degradation of organic pollutants, Chemosphere, 151 (2016) 280–288.
[9] A.R. Khataee, M. Fathinia, S.W. Joo, Simultaneous monitoring of photocatalysis of three pharmaceuticals by immobilized TiO_2 nanoparticles: chemometric assessment, intermediates identification and ecotoxicological evaluation, Spectrochim. Acta, Part A, 112 (2013) 33–45.
[10] S. Fathinia, M. Fathinia, A.A. Rahmani, A. Khataee, Preparation of natural pyrite nanoparticles by high energy planetary ball milling as a nanocatalyst for heterogeneous Fenton process, Appl. Surf. Sci., 327 (2015) 190–200.
[11] C.D. Qi, X.T. Liu, C.Y. Lin, X.H. Zhang, J. Ma, H.B. Tan, W. Ye, Degradation of sulfamethoxazole by microwave-activated persulfate: kinetics, mechanism and acute toxicity, Chem. Eng. J., 249 (2014) 6–14
[12] Y.J. Li, B.J. Zhang, X.L. Liu, Q. Zhao, H.M. Zhang, Y.C. Zhang, P. Ning, S.L. Tian, Ferrocene-catalyzed heterogeneous Fenton-like degradation mechanisms and pathways of antibiotics under simulated sunlight: a case study of sulfamethoxazole, J. Hazard. Mater., 353 (2018) 26–34.
[13] M. Bayat, M. Sohrabi, S.J. Royaee, Degradation of phenol by heterogeneous Fenton reaction using Fe/clinoptilolite, J. Ind. Eng. Chem., 18 (2012) 957–962.

[14] Y. Alegría, F. Liendo, O. Núñez, On the Fenton Degradation Mechanism. The Role of Oxalic Acid, Aekivoc, 10 (2003) 538.
[15] Hermosilla, Daphne, M. Cortijo, C.P. Huang, Optimizing the treatment of landfill leachate by conventional Fenton and photo-Fenton processes, Sci. Total Environ, 407 (2009) 3473–3481.
[16] A. Akyol, O.T. Can, E. Demirbas, M. Kobya, A comparative study of electrocoagulation and electro-Fenton for treatment of wastewater from liquid organic fertilizer plant, Sep. Purif. Technol., 112 (2013) 11–19.
[17] R. Rodríguez, J.J. Espada, M.I. Pariente, J.A. Melero, F. Martínez, R. Molina, Comparative life cycle assessment (LCA) study of heterogeneous and homogenous Fenton processes for the treatment of pharmaceutical wastewater, J. Cleaner Prod., 124 (2016) 21–29.
[18] Y.W. Xie, L.J. Chen, R. Liu, Oxidation of AOX and organic compounds in pharmaceutical wastewater in RSM-optimized-Fenton system, Chemosphere, 155 (2016) 217–224.
[19] P. Bautista, A.F. Mohedano, M.A. Gilarranz, J.A. Casas, J.J. Rodriguez, Application of Fenton oxidation to cosmetic wastewaters treatment, J. Hazard. Mater., 143 (2007) 128–134.
[20] M. Nurbas, S.B. Kutukcuoglu, Investigation of water decolonization by Fenton oxidation process in batch and continuous systems, Desal. Wat. Treat., 55 (2015) 3731–3736.
[21] N. Biglarijoo, S.A. Mirbagheri, M. Ehteshami, S.M. Ghaznavi, Optimization of Fenton process using response surface methodology and analytic hierarchy process for landfill leachate treatment, Process Saf. Environ., 104 (2016) 150–160.
[22] J.A.D.L. Perini, M. Perez-Moya, R.F.P. Nogueira, Photo-Fenton degradation kinetics of low ciprofloxacin concentration using different iron sources and pH, J. Photochem. Photobiol., A, 259 (2013) 53–58.
[23] J. Feng, X. Hu, P.L Yue, Effect of initial solution pH on the degradation of Orange II using clay-based Fe nanocomposites as heterogeneous photo-Fenton catalyst, Water Res., 40 (2006) 641–646.
[24] J.A. Zazo, G. Pliego, S. Blasco, J.A. Casas, J.J. Rodriguez, Intensification of the Fenton process by increasing the temperature, Ind. Eng. Chem. Res., 50 (2015) 866–870.
[25] E. Kan, S.G. Huling, Effects of temperature and acidic pre-treatment on Fenton-driven oxidation of MTBE-spent granular activated carbon, Environ. Sci. Technol., 43 (2009) 1493.
[26] O.K. Ince, M. Ince, V. Yonten, A. Goksu, A food waste utilization study for removing lead(II) from drinks, Food Chem., 214 (2017) 637–643.
[27] C.C. Yoong, C.N. Ling, Y.Y. Aniza, R.A. Talib, L.C. Lim, Optimization of total phenolic content extracted from *Garcinia mangostana* Linn. Hull using response surface methodology versus artificial neural network, Ind. Crop. Prod., 40 (2012) 247–253.
[28] T. Xu, Y. Liu, F. Ge, L. Liu, Y. Ouyang, Application of response surface methodology for optimization of azocarmine B removal by heterogeneous photo-Fenton process using hydroxy-iron–aluminum pillared bentonite, Appl. Surf. Sci., 280 (2013) 926–932.
[29] G. Chen, J. Chen, C. Srinivasakannan, J.H. Peng, Application of response surface methodology for optimization of the synthesis of synthetic rutile from titania slag, Appl. Surf. Sci., 258 (2012) 3068–3073
[30] M.M. Song, C. Branford-White, H.L. Nie, L.M. Zhu, Optimization of adsorption conditions of BSA on thermosensitive magnetic composite particles using response surface methodology, Colloids Surf., B, 84 (2011) 477–483.
[31] A.A. Salarian, Z. Hami, N. Mirzaei, S.M. Mohseni, A. Asadi, H. Bahrami, M. Vosoughi, A. Alinejad, M.R. Zare, N-doped TiO_2 nanosheets for photocatalytic degradation and mineralization of diazinon under simulated solar irradiation: optimization and modeling using a response surface methodology, J. Mol. Liq., 220 (2016) 183–191.
[32] Z.M. Shaykhi, A.A.L. Zinatizadeh, Statistical modeling of photocatalytic degradation of synthetic amoxicillin wastewater (SAW) in an immobilized TiO_2 photocatalytic reactor using response surface methodology (RSM), J. Taiwan Inst. Chem. Eng., 45 (2014) 1717–1726.
[33] A.V. Schenone, L.O. Conte, M.A. Botta, O.M. Alfano, Modeling and optimization of photo-Fenton degradation of 2,4-D using ferrioxalate complex and response surface methodology (RSM), J. Environ. Manage., 155 (2015) 177–183.
[34] M. Fayazi, D. Afzali, M.A. Taher, A. Mostafavi, V.K. Gupta, Removal of Safranin dye from aqueous solution using magnetic mesoporous clay: optimization study, J. Mol. Liq., 212 (2015) 675–685.
[35] A. Eslami, A. Asadi, M. Meserghani, H. Bahrami, Optimization of sonochemical degradation of amoxicillin by sulfate radicals in aqueous solution using response surface methodology (RSM), J. Mol. Liq., 222 (2016) 739–744.
[36] B.G. Kwon, D.S. Lee, N. Kang, J. Yoon, Characteristics of *p*-chlorophenol oxidation by Fenton's reagent, Water Res., 33 (1999) 2110–2118.
[37] W.Z. Tang, C.P. Huang, 2,4-Dichlorophenol oxidation kinetics by Fenton's reagent, Environ. Technol., 17 (1996) 1371–1378.
[38] J.J. Pignatello, Dark and photoassisted iron (3+)-catalyzed degradation of chlorophenoxy herbicides by hydrogen peroxide, Environ. Sci. Technol., 26 (1992) 944–951.
[39] C. Höfl, G. Sigl, O. Specht, I. Wurdack, D. Wabner, Oxidative degradation of AOX and COD by different advanced oxidation processes. A comparative study with two samples of a pharmaceutical wastewater, Water Sci. Technol., 35 (1997) 257–264.
[40] M.A. Wei, Fundamental Research on Flotation Separation of Chalcopyrite and Galena, College of Resources and Civil Engineering, Northeastern University, Shenyang, China, 2008.
[41] Y.Q. Sun, Y.Z. Hu, Analytical Chemistry, 2nd ed., Science Press, Beijing, China, 2006, p. 271.
[42] D.H. Liu, C. Ma, G.H. Gu, C.Q. Wang, X. Chen, Removal of isopropyl ethylthionocarbamate from aqueous solution by oxidation, Desal. Wat. Treat., 72 (2017) 228–234.
[43] R. Chen, J. Pignatello, Role of quinone intermediates as electron shuttles in Fenton and photo assisted Fenton oxidations of aromatic compounds, Environ. Sci. Technol., 31 (1997) 2399–2406.
[44] C. Liang, C.P. Liang, C.C. Chen, pH dependence of persulfate activation by EDTA/Fe(III) for degradation of trichloroethylene, J. Contam. Hydrol., 106 (2009) 173–182.
[45] S. Rodriguez, L. Vasquez, D. Costa, A. Romero, A. Santos, Oxidation of Orange G by persulfate activated by Fe(II), Fe(III) and zero valent iron (ZVI), Chemosphere, 101 (2014) 86–92.

Supplementary information:

- Before the RSM experiment, single-factor experiment is firstly conducted to determine the range of the values. Results are shown in Figs. S1–S3.

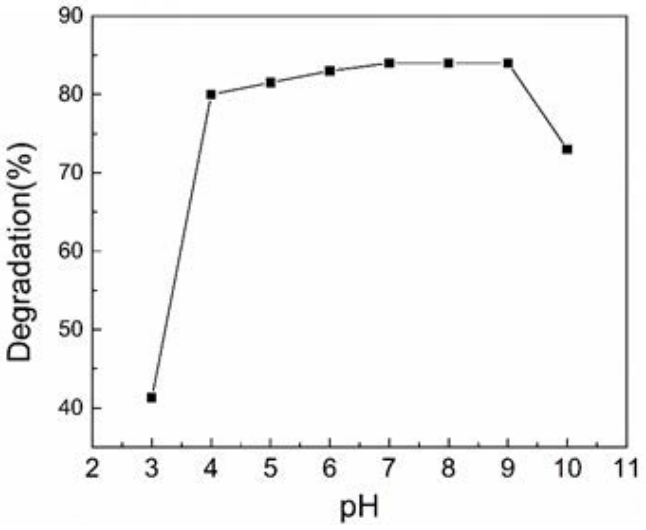

Fig. S1. Effect of the initial solution pH on the Z-200 degradation in Fenton process. $[Z\text{-}200]_0$ = 20 mg/L, $[Fe^{2+}]_0$ = 120 mg/L, $[H_2O_2]_0$ = 150 mg/L.

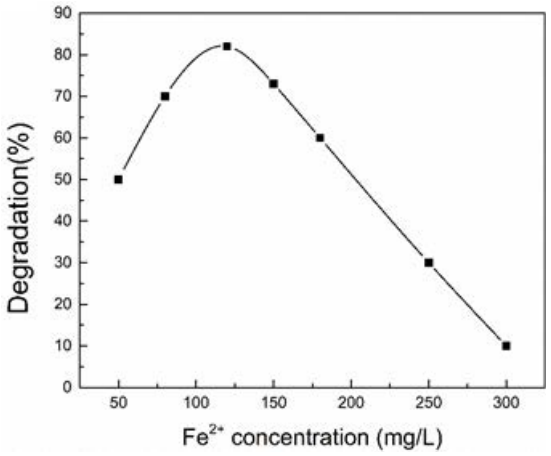

Fig. S2. Effect of Fe^{2+} concentration on the Z-200 degradation in Fenton process. $[Z\text{-}200]_0$ = 20 mg/L, pH = 6.7, $[H_2O_2]_0$ = 150 mg/L.

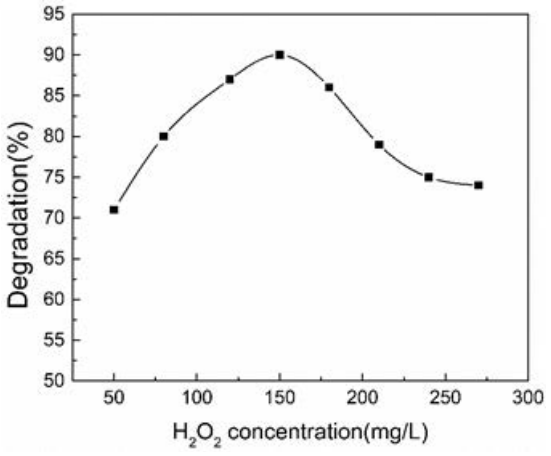

Fig. S3. Effect of H_2O_2 concentration on the Z-200 degradation in Fenton process. $[Z\text{-}200]_0$ = 20 mg/L, $[Fe^{2+}]_0$ = 120 mg/L, pH = 6.7.

- Figs. S4 and S5 are the UV spectrum of Z-200 and Standard working curve, respectively.

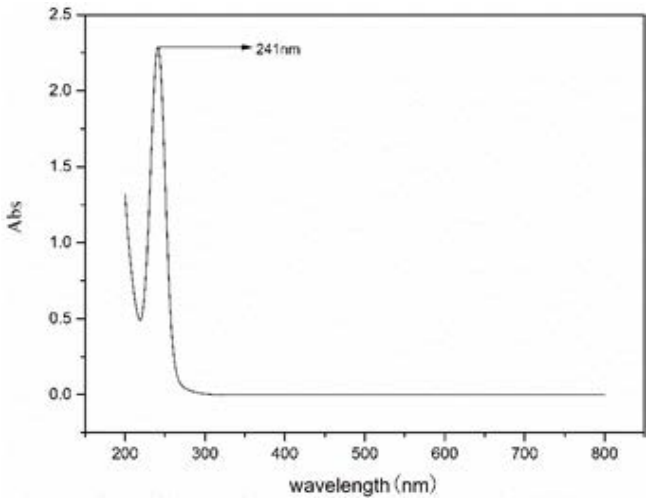

Fig. S4. The UV spectrum of Z-200.

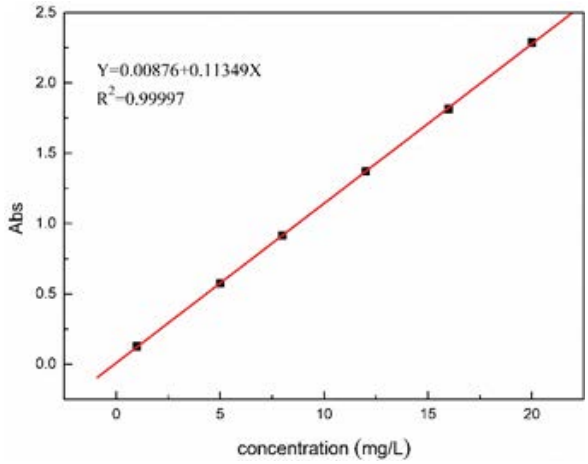

Fig. S5. Standard working curve.

- Mass spectrums of each peak in the TIC are shown in Figs. S6 (compound A), Fig. S7 (compound B), Fig. S8 (compound C), Fig. S9 (compound D), Fig. S10 (compound E), Fig. S11 (compound F), Fig. S12 (compound G), and Fig. S13 (compound H).

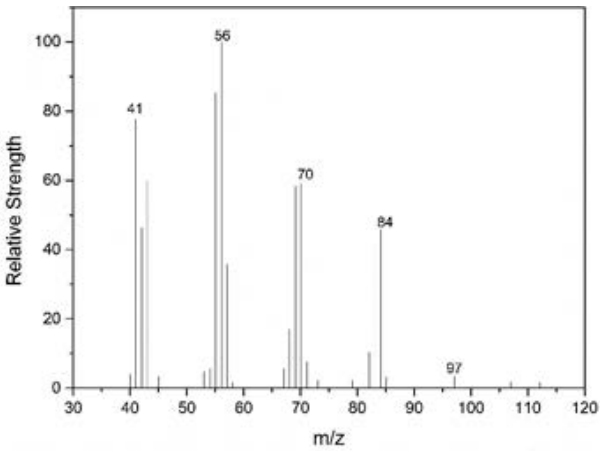

Fig. S6. MS spectrums of compound A.

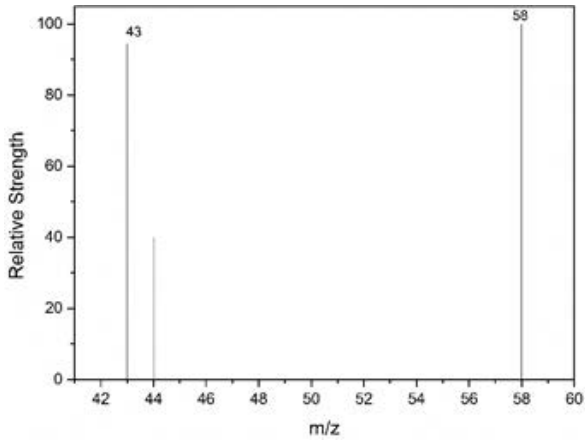

Fig. S7. MS spectrums of compound B.

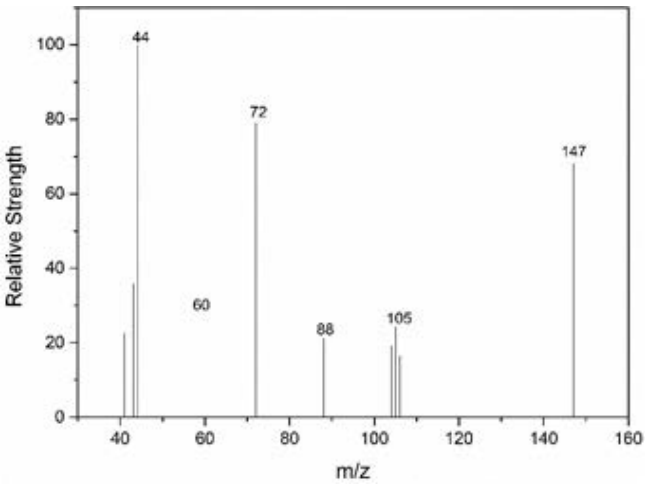

Fig. S8. MS spectrums of compound C.

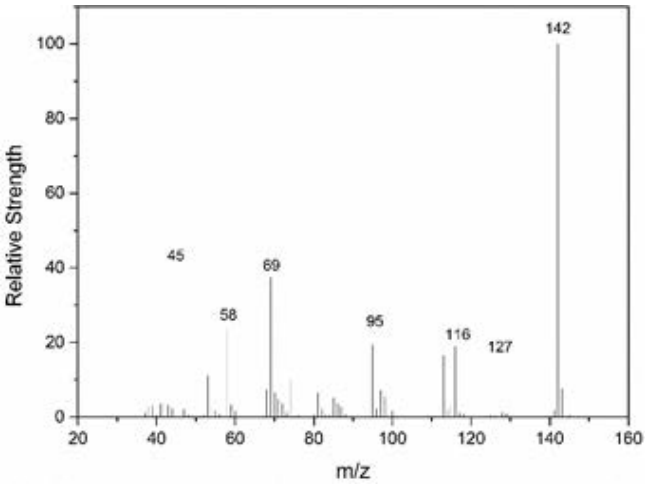

Fig. S9. MS spectrums of compound D.

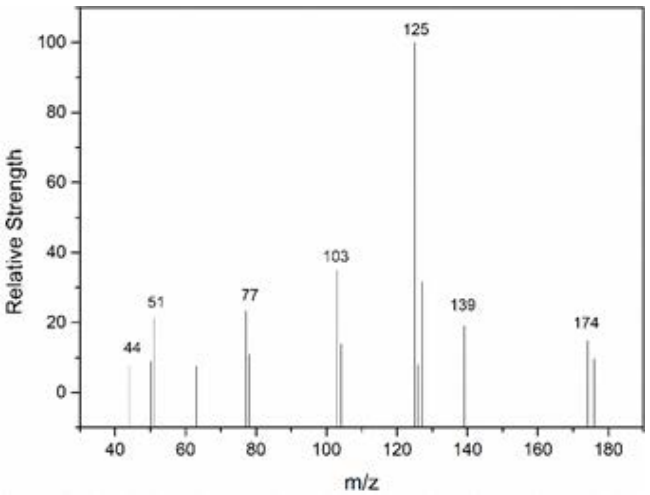

Fig. S10. MS spectrums of compound E.

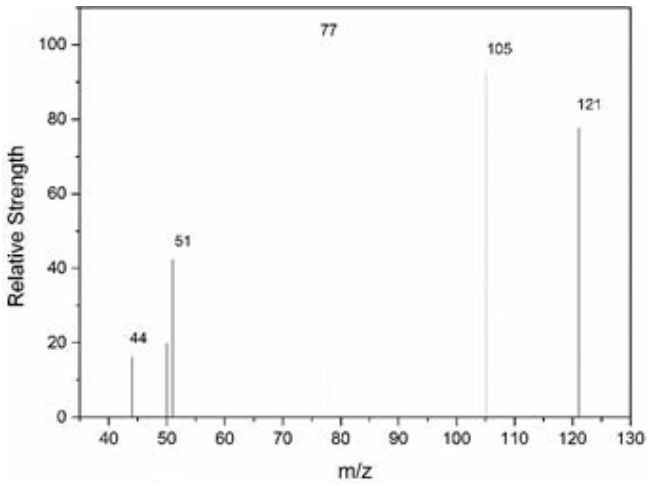

Fig. S11. MS spectrums of compound F.

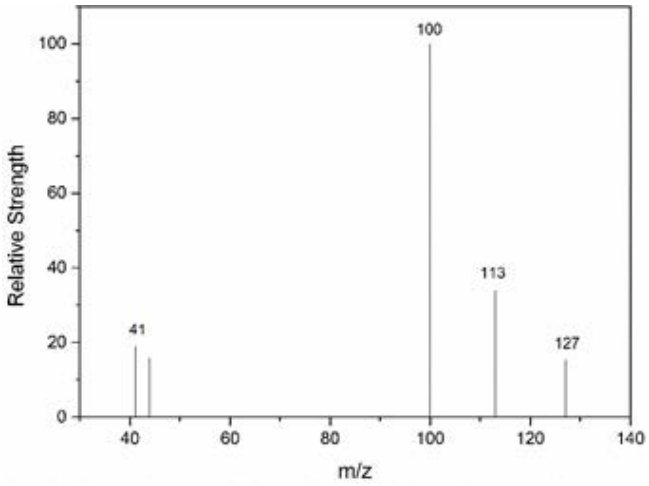

Fig. S12. MS spectrums of compound G.

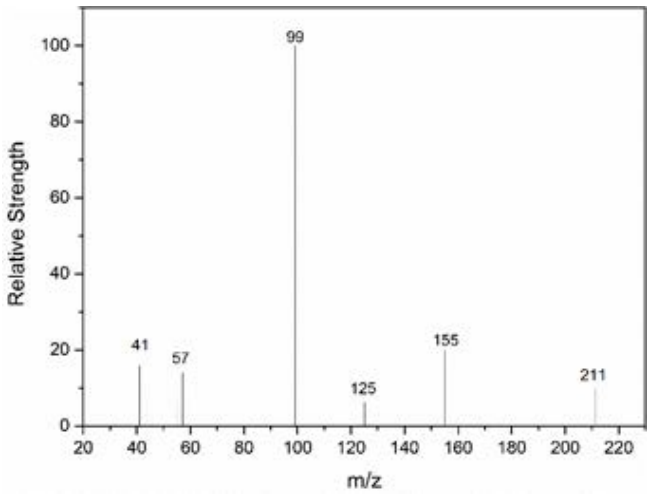

Fig. S13. MS spectrums of compound H.